Discussion

The Riverina deposit contains beryl in a range of colours. Blue and colourless beryl crystals were observed within friable feldspar-quartz and medium to dark green emerald beryl was hosted within phlogopite schist rock. All colour variants of beryl, with the exception of blue, were also observed in massive quartz material together with aggregated phlogopite mica.

Beryl formed initially in the pegmatite and is blue coloured; this generation was observed to be poorly formed and often massive and its felsic host rock deeply altered. Another generation of beryl formed in the phlogopite schist; this is the site of the emerald variety with medium to dark green colour due to the addition of the chromophore, chromium. However, colourless beryl crystals also occur in the phlogopite schist. Emerald crystals developed within phlogopite schist that had resulted from K-metasomatism of mafic minerals as narrow zones bounding pegmatites. The pegmatite had limited mineralogy; principally containing quartz, alkali feldspar and beryl. No other pegmatite-hosted minerals have been noted at Riverina with the exception of rare tourmaline (Garstone, 1981), one report of a topaz specimen (Jacobson et al., 2007) and phenakite (Fetherston et al., 2017). None of these minerals were found by the authors from samples taken at the sorting plant.

Regional structural deformation and alteration has affected all generations of beryl. There are several indications of growth stresses in the emerald crystals. These include: the phlogopite mica host rock has a fine crenulated pattern of kinked schistosity; emerald crystals are highly fractured and have infillings of phlogopite mica within fractures as they developed and widespread fracturing of the emerald crystals and stresses that resulted in the biaxiality of the optic figure and zones of anisotropy of the emerald. A generation of secondary micro-quartz also occupies fractures within emerald crystals. Other features of late formation events are dissolution and etching of crystals and epigenetic mineralisation that has infilled some tubular growth inclusions in the emerald. Colour zoning shown by both blue beryl and emerald at Riverina indicate ongoing and persistent change in the availability of the chromophore, chromium. The felsic rocks are all highly decomposed and discrete patches of unaltered feldspar are rare.

The range of surface textures observed on emerald crystals indicates their formation under different conditions; some crystals have smooth unblemished faces with high lustre and others are textured by the imprinting of host rock contact minerals. The crystals are highly fissured and many fractures are infilled by, as well as enveloped by, black phlogopite mica.

Metasomatic alteration of country rock mafic and ultramafic lavas has resulted in the formation of narrow localised zones of phlogopite mica schist within which porphyroblasts of coloured-zoned emerald crystallised. Variation of the intensity of green colouration of the beryl is ascribed by Garstone (1981) to the period that beryllium and alkali-enriched fluids have reacted with the chrome-bearing ultramafic rocks. Emerald crystals are the result of contact metasomatism by the complex interaction of pegmatitic, hydrothermal and pneumatolytic processes (Garstone 1981, Jacobson et al., 2007).

These multiphase events indicate a complex growth environment for the emerald in which their primary growth features have been overprinted and strongly influenced by secondary events involving deformational stress, fracture-infilling and some epigenetic mineralisation.

Acknowledgements

The Directors of Australian Menzies Emerald Pty. Ltd. permitted the authors to visit the Riverina emerald workings for a few days during May 2016. They also supplied a parcel of specimens, uncut stones of varying dimensions and some faceted emeralds for examination.

Photographs for Figures 3, 4, 5, 6 supplied by B. Macray; those for Figures 2, 7, 8, 9,10, 11, 12, 13, 16, 17, 18, 19, 21, 22, 23 supplied by S. Stocklmayer.

REFERENCES

Clark, P. (2001) The Riverina Emerald Deposit. *Mineral Society of Western Australia Newsletter*, **2**(6), pp. 3-5.

Fetherston, J.M., Stocklmayer, S.M., Stocklmayer, V.C. (2017) *Gemstones of Western Australia*. (2nd Edition). Geological Survey of Western Australia, Mineral Resources Bulletin 25, pp. 39.

Garstone, J.D. (1977) *Emerald and green beryl mineralization at Riverina Station near Menzies, Western Australia*. University of Western Australia, BSc (Honours) thesis (unpublished).

Garstone, J.D. (1981) The geological setting and origin of emeralds from Menzies, Western Australia. *Journal of the Royal Society of Western Australia*, **64**, pp. 53-64.

Graindorge, J.M. (1974) A gemmological study of emerald from Poona, Western Australia. *The Australian Gemmologist*, **12**(2), pp. 75-80.

Groat, L.A. (2007) The geology of gem deposits. *Mineralogical Association of Canada*. Short Course Series, Vol. **37**. The University of British Columbia, pp. 82- 270.

Jacobson, M.I., Calderwood, M.A., Grguric, B.A. (2007) *Guidebook to the pegmatites of Western Australia*. 348-352 pp. Hesperian Press: Carlisle, Western Australia.

Lindsay, R. (2000) Menzies emeralds: *Timeless treasures from the Australian outback*. 14 p. Kalgoorlie. Unpublished

Marshall D., Downes P.J., Elli S., Greene R., Loughrey L., Jones P. (2016) Pressure–Temperature–Fluid Constraints for the Poona Emerald Deposits, Western Australia: Fluid Inclusion and Stable Isotope Studies. *Minerals*, **6**(130); doi:10.3390/min6040130 www.mdpi.com/journal/min6040130 www.mdpi.com/journal/minerals

Mindat.org accessed September 2017.

MINEDEX. Mines and Minerals database. Accessed September 2017 Western Australia Geological Survey.

Mumme, I.A. (1982) *The Emerald*. 76-68 pp. Mumme Publications: Port Hacking

Ostwald, J. (1964) On the microstructures and origin of emerald. *The Australian Gemmologist*, **6**(35), pp 7-10.

Prospect, (2004) Emeralds: the envy of many. Western Australia Department of Industry and Resources, *Prospect magazine*, June-August. p. 12.

Schwarz, D. (1991) Australian Emeralds. The Australian Gemmologist, **17**(12), pp. 488-497.

Schwarz, D., Giuliani, G., Grundmann, G., Glas, M. (2002) The origin of emerald. In *Emeralds of the world*; ExtraLapis v.2, Lapis International. 100 p. LLC: East Hampton.

W.A. Gem News (1975) October Field Trip – Menzies Emeralds. In *W.A. Gem News*; newsletter, October. p. 3.

Whitfield G.B. (1975) Emerald Occurrence near Menzies Western Australia. *The Australian Gemmologist*, **12**(5), pp. 150-152.

Zwaan, J.C., Seifert, A.V., Vrana, S., Laurs, B.M., Ancker, B., Simmons, W.B., Falster, A.U., Lustenhouwer, W.J., Muhlmeister, S., Koivula, J.I., Garcia-Guillerminet, H. (2005) Emeralds from the Kafubu Area, Zambia. *Gems and Gemology*, **41**(2), pp. 116-148.

Investigation of the porosity of some opaline siliceous materials

Grant Pearson, Dip Gem FGAA GR003
grantpearson@optusnet.com.au

Abstract: The microstructures of a limited selection of porous silica materials, including natural gem opals from several sources, were examined and the possible origins and extents of their porosities were compared. The investigation centred on characterising Ethiopian opal which often displays sufficient open porosity to be significantly absorbent. This can even lead to its soiling and loss of desirability for jewellery purposes. Alternatively, the accessible porosity offers an opportunity for colour-enhancement staining. A provisional procedure was developed for assessing the relative extent of the open porosity by water displacement and a range of the porous materials was evaluated. The procedure enabled the determination of the densities of the various silicas as a quantitative property of their nature, and also determined the spontaneous thermal adsorption and desorption of moisture from the atmosphere which is considered to possibly influence subsequent crazing propensities. Porosity or surface-accessible voidage ranged from effectively nil to in excess of 38% by volume. Apparent silica densities ranged from 1.92 to 2.49 g/cm^3.

Key Words: silica, opal, Ethiopia, Mexican, absorption, hydrophane, voidage, porosity, diffraction, volcanic

Figure 1. Left: Ethiopian Shewa brown opal nodule and hydrophane coating with intense POC that instantly disappears upon partial moistening. Right: It reappears when dry. Nodule approximately 30 mm diameter.

Introduction

Silica occurs widely as a natural mineral in a number of different guises, including quartz, mogánite, keatite, cristobalite, tridymite, lechatelierite, coesite and stishovite. The amorphous naturally hydrous gel-variety known as opal is a secondary silica mineral(oid) of aqueous origin and it may develop a play of colour (POC) by coherent diffraction from a regularly packed array of equi-sized silica spheroids. "Opalite", i.e. the naturally occurring amorphous silica mineral(oid) and not the man-made glass imitation bearing the same name, and "hyalite" or the glassy "volcanic" or "sinter" opal (known often as Müller's glass) do not usually show a POC and are generally colourless and transparent to opaque.

The regularly packed silica spheroids of gem-opal POC arrays (Sanders, 1964; 1968) mimic, in the visible range, the much smaller scale of three-dimensional regularly packed arrays of atoms in crystalline atomic and molecular lattices. These display coherent diffraction of specific wavelengths according to the Bragg criterion (Cullity, 1959; Nassau, 1983). Gem opal with a vitreous (glassy) consistency and an attractive POC has long been highly valued for its captivating spectral colour patterning and for adornment purposes. This is in spite of its gemmological disadvantages of relative softness (about Mohs 6), fragility and its frequent instability attributable to surface dehydration and localised shrinkage causing spontaneous crazing and cracking. Water content is variable from less than about 5% to more than 10% by weight. Some reports of water content in natural opal suggest values up to 35% (Todor, 1976), although Australian gem opal generally has total water content between about 5 and 8% (Pearson, 1985).

Opal structure

Gem-quality opal displaying a POC is composed of regularly stacked layers of silica spheroids leaving voidage or vacant-volume between the spheres, unless it has been subsequently infilled with silica gel. This gel must necessarily be of a slightly different refractive index (RI) to the spheroid array, or the scattering of light leading to the POC cannot occur (Sanders and Darragh, 1971).

World opal occurrence

Significant deposits of opal, often with an intense POC, were discovered in Ethiopia in the 1990s, initially in the Shewa Province, where nodules of dark reddish-brown opal encased in clay were found (Figure 1).

Figure 2. Ethiopian Welo opal fragments with POC, used for porosity testing.

Figure 3. Ethiopian Shewa gem-opal nodule, naturally-fractured due to intrinsic internal stress.

Figure 4a. Selection of sawn Ethiopian Shewa white, grey and brown banded potch-opal nodules.

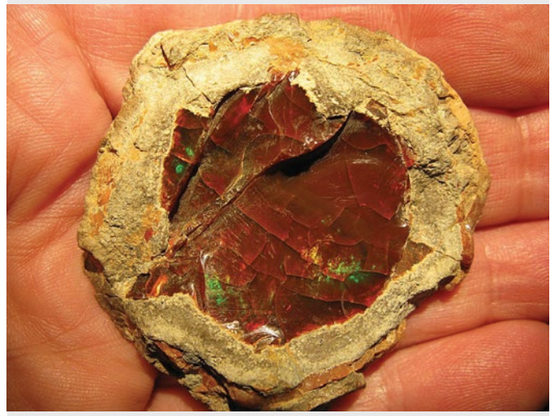

Figure 4b. Left: Fractured and sawn Shewa brown opal nodule with moderate intensity of POC.

Figure 4c. Right: Transmitted light through the sawn slice of Shewa nodule of Figure 4b showing the fracture network generated by pre-existing stress, probably induced by porosity dehydration and shrinkage.

More recently, another Ethiopian deposit has been located in Welo (also called Wello, Wollo) Province. This material is generally much paler and sometimes almost white often with a strong POC (Figure 2). Both the Shewa and Welo materials have been shown at times to be significantly porous and absorbent.

The recently exploited pale gem opal in Ethiopia from the Welo Province in particular, possesses substantial porosity. However, historically, such porous "hydrophane" opals have only been rare curiosities and of little commercial significance (Rondeau et al., 2010). The opal from the earlier exploited deposits in Shewa Province Ethiopia occurs as dark-brown nodules with a POC in spheroidal cavities in weathered volcanic debris (Hoover et al., 1996) (Figures 3 and 4a-c).

Although the Shewa material has not often been observed to be appreciably porous or absorbent, perhaps indicating only minimal interconnected voidage rather than inaccessible closed and isolated cavities, the author's first observation of Ethiopian hydrophane opal from this location was a thin white chalky film of moisture-absorbent opal with an intense POC. It enclosed a translucent and non-absorbent glassy opal core with only a weak POC. Moistening the thin chalky layer caused immediate disappearance of the POC, which reappeared when the layer dried out moments later (Figure 1).

Figure 5. Javanese (Indonesia) polished hydrophane grey and black ("tea") opals.

Figure 6. "Bohemian" cachalong, absorbent chalky non-gem opaline silica, Czech Republic.

Figure 7. Volcanic opal nodule with banded POC, Spencer, Idaho.

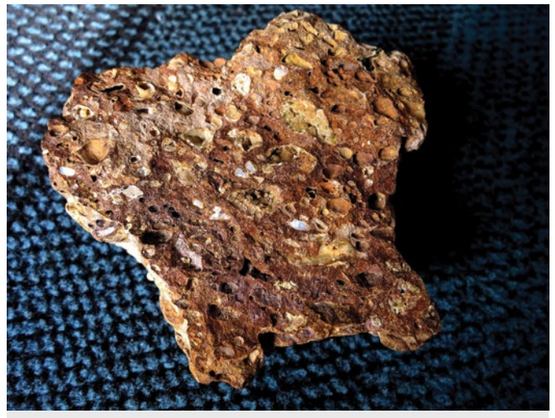

Figure 8a and b. Weathered volcanic scoria from Rocky Bridge Creek, NSW, containing small (non-commercial) gem-opal and also associated hyalite-opal nodules in adjoining vughs. The specimen measures approximately 10 cm across. Figure 8b is a close-up photo of this specimen.

Examples of hydrophanes have been recovered from Indonesia (Figure 5) (Sun et al., 2009). Non-commercial hydrophane examples have also been recovered from some minor occurrences in the USA, such as Rainbow Ridge, Nevada (wood-opal), as well as in the present-day Czech Republic ("Bohemia"), where "Bohemian" cachalong opal has been recovered. Cachalong opal is a non-gem chalky-white variety and reputedly highly absorbent opaline silica, apparently usually occurring as botryoidal layers on igneous host rocks (Figure 6).

Opal from various other locations in the USA has not been observed to show porosity, and is essentially glassy and non-absorbent, such as from Spencer in the Snake River Valley (Idaho), where a gem-quality volcanic opal with a layered POC occurs as hemi-spheroidal amygdules in weathered volcanic debris and ash (Figure 7). Specimens of this material were earlier provided to the author by the miner (L. Enos, California) and then passed to Dr J. V. Sanders for electron microscopy in the 1970s.

Most Australian opal is non-porous and formed in ancient sedimentary rocks by water permeation from the edge of the Great Artesian Basin, rather than by the more usual groundwater percolating through active silica in volcanic eruption debris (Darragh and Sanders, 1969). There are a number of non-commercial Australian "volcanic" opal occurrences with a POC. However, that opal is not truly volcanic in the sense that it is itself not magmatic but is a secondary emplacement (Darragh and Sanders, 1969). Locations include Mount Bougrom, Tooraweena, Rocky Bridge Creek, Mullumbimby and Tintinbar in NSW, although no hydrophane has been reported at these sites. Photomacros of precious opal amygdules in vesicles of volcanic scoria from Rocky Bridge Creek are shown with small hyalite opal nodules in an adjoining vugh (Figures 8a and b).

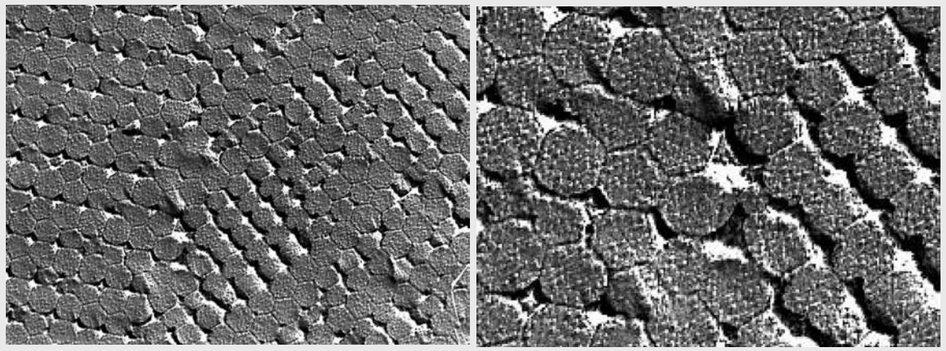

Figure 9a and b. Left: Javanese ("volcanic") opal displaying various packing configurations, including zones of close-packing and simple-cubic, as well as instances of packing defects including spheroid compression into polyhedroids, grain boundaries, vacancies, interstitials and twinning.

Right: Inspection of this enhanced and magnified image reveals that the diffracting-array spheroids are composed of randomly aggregated primary micro-spheroids, unlike much Australian opal where the diffraction array spheroids are composed of concentric layers of primary microspheroids (see Figure 10a and b of some Coober Pedy Australian opal).

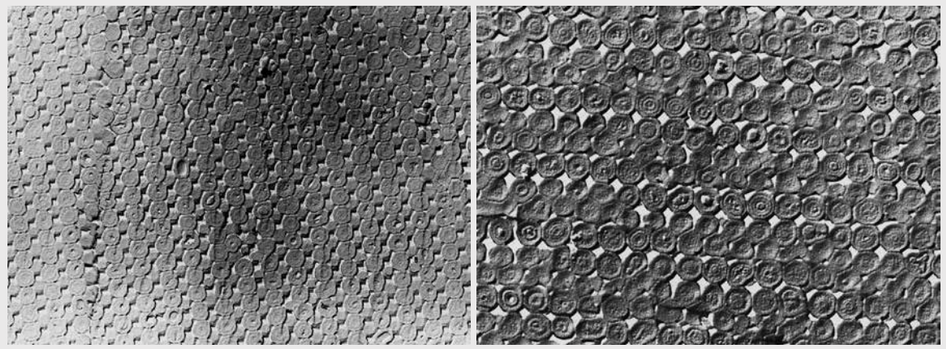

Figure 10a and b. Left: Coober Pedy Australian ("sedimentary" Desert Sandstone Series) opal with POC, showing the same types of packing defects as in Javanese opal (Figure 9a and b), and also the concentric shell-layering of the primary microspheroids constructing the spheroids that comprise the visibly-diffracting array.

Right: Magnified image showing concentric shells of primary microspheroids.

The nature of the original deposits of opal, reaching back to Roman times, i.e. Dubnik and Cervenica (earlier in Hungary) is uncertain, and some of that material has been reported to be hydrophane (Semrad, 2011). However, some of it was considered to be unstable developing dehydration crazing upon exposure after its recovery (Semrad, 2015), implying *a* water content within voidage. The factors that determine whether a specific opal is hydrophane and absorbent, or becomes water impervious and "glassy", are obscure.

Opal "A", "C", "CT"

Natural hydrous silicas have also been examined by X-ray diffraction, and it was suggested that they can be classified into at least three micro-structural categories, including "A", "C", and "CT". These designations, based on experiments by Jones and Segnit (1971), indicate significant proportions respectively of highly-disordered and amorphous silica ("A") representing most opal, a well-ordered α-cristobalite ("C"), as well as a disordered α-cristobalite/α-tridymite ("CT") phase. These differences suggest that the microstructural compositions of opal from different locations may not be uniformly homogeneous, and may contain different proportions of crystallinity depending upon factors such as age, depth and temperature of origin, and environmental geology. These could then significantly influence physical properties including ease of hydration and dehydration, and microstructural ordering and porosity (Jones and Segnit, 1971; Jones et al., 1964).

The nature and disposition of the water within opal has also been examined by Jones and Segnit (1969).The infrared spectra and dilatometric curves of progressively thermally dehydrated opal specimens, suggested that much of the contained water was present as intrinsic hydroxyl groups bound to the silica ("silanol"). The amount of water was considered to be inconsistently large relative to the surface area of the spheres comprising the diffracting array, where it was inferred to be located by adsorption. It was then shown that the diffracting array spheres were themselves composed of very much smaller primary spheres, often arranged randomly as particularly demonstrated in Indonesian Javanese opal (Figures 9a and b). Alternatively they were arranged in concentric shells, such as in Australian opal from Coober Pedy (Figures 10a and b), to generate the larger composite spheres of the diffracting arrays (Sanders and Darragh, 1971). The large additional surface area of these primary microspheres accounted for the higher than expected combined water content, as the silanol hydroxyl functions (Jones and Segnit, 1969).

Note: the transmission electron microscope (TEM) replica images reproduced in this paper are all more than 30 years old, available now only as A4 monochrome prints in the author's possession. All were taken by Dr J.V. Sanders, (or his assistant at the time, Bramwell Dawson) who then bequeathed all these records to the author, as noted in the acknowledgements. The make and model of the EM is not known, (it was located in the long disbanded Tribophysics Department building then on the Melbourne University campus). Any magnification indications were simply casually noted by pen in the photo-print margins as "40,000x" for example (and sometimes not even at all), so that actual magnifications such as relative to the initial negative before cropping and printing are obviously uncertain. Since the images are of opal, mostly with a POC, a size indication may be available from the spheroid sizes which lie mostly between about 300 nm and typically 600 nm diameter for visible diffraction.

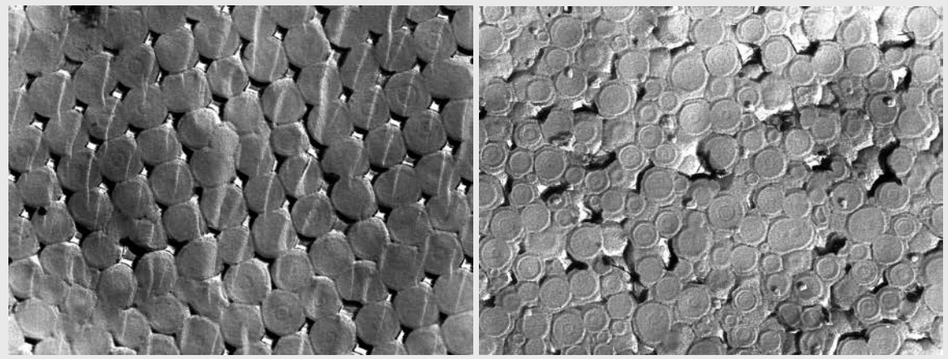

Figure 11. Left: Spencer, Idaho gem-quality opal with POC, showing predominantly simple cubic ordering of spheroids, each developed by concentric layering of smaller primary spheroids, and with minor zones of close-packing associated also with spheroid-compression into polyhedroids and their reduced interspheroid-voidage. Also observable are examples of "crystal defect" ordering structures including interstitials, vacancies, grain boundaries, etc.

Figure 12. Right: Spencer, Idaho potch (opaque white) opal without POC, due to variably sized spheres, also developed by concentric layering of smaller primary spheres, causing irregular disordered packing and incoherent light scattering from randomly dispersed voidage cavities.

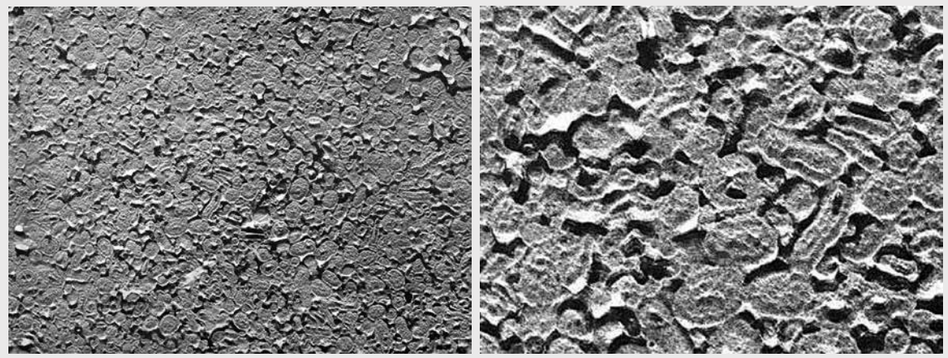

Figure 13a and b. Common-opal or "potch" without POC, of misshapen non-spheroidal particles, developing random packing with negligible inter-particle voidage. Spencer, Idaho.

Ideal sphere packing densities considerations

The extent of vacant-voidage can differ substantially in different theoretical packing sequences of equally-sized rigid spheres depending on the configuration of the sphere stacking (Moffatt et al., 1964).

Using only the simple formula for the volume of a sphere, i.e. $V=4\pi r3/3$, and Pythagoras' Theorem that the square of the length of the hypotenuse (h) of a right-angled triangle (i.e. the side opposite the right angle), is equal to the sum of the squares of the lengths of the two other sides (a and b) at right-angles, i.e. $h^2 = (a^2 + b^2)$, the extents of theoretically ideal voidage can be easily calculated. A face-centred-cubic (FCC) lattice is close-packed, i.e. it is at the maximum known density obtainable of equi-sized spheres inside the cubic structure where each sphere is sitting in the cusp of the three spheres below it, and the proportion of its idealised cubic unit-cell volume occupied by the rigid spheres just touching each other is

$(\pi/3\sqrt{3})$ or 74.05%. For the similar but rather less closely packed body-centred-cubic (BCC) structure it is $(\pi\sqrt{3}/8)$ or 68.02%, and for simple cubic packing which is even less densely packed, it is $(\pi/6)$ or 52.36%. A domain of simple cubic packing can be seen in Figure 11. Conversely, the theoretically-ideal vacant-voidages are respectively (100-74.05) = 25.85% for FCC, 31.88% for BCC, and 47.64% for the simple cubic sequence. Hexagonal close packing (HCP) is actually identical to FCC, except that every third layer of spheres is just displaced sideways only one sphere, so that the extent of voidage is necessarily identical to FCC, and HCP is the only other maximum density packing sequence known (Gardner,1960).

More randomly packed irregular arrays, due to inclusion of misshapen or variably-sized spheres, can develop even greater voidage (Figure 12), although the converse may also occur when smaller irregular particles can fill much of the interspheroidal volume (Figure 13a and b, Spencer potch).

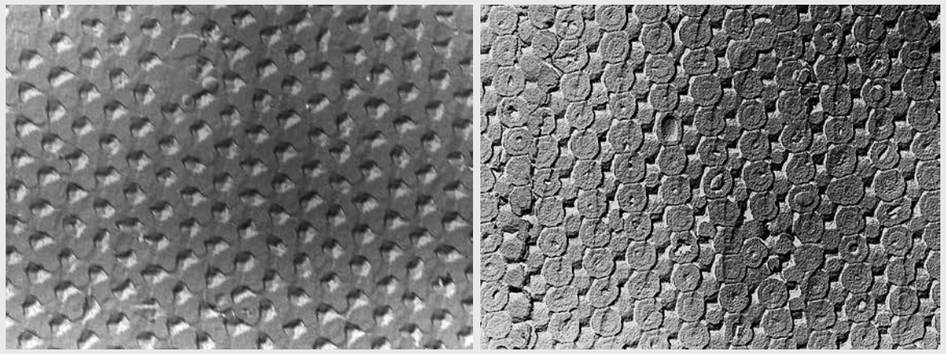

Figure 14. Left: Closed and isolated pore-cavity content in a sample of dark opal from the Coocoran field, Lightning Ridge, NSW.

Figure 15. Right: Interconnected pore-voidage in a sample of dark opal showing a planar fracture apparently across a BCC [100] plane, also from the Coocoran field, Lightning Ridge, NSW.

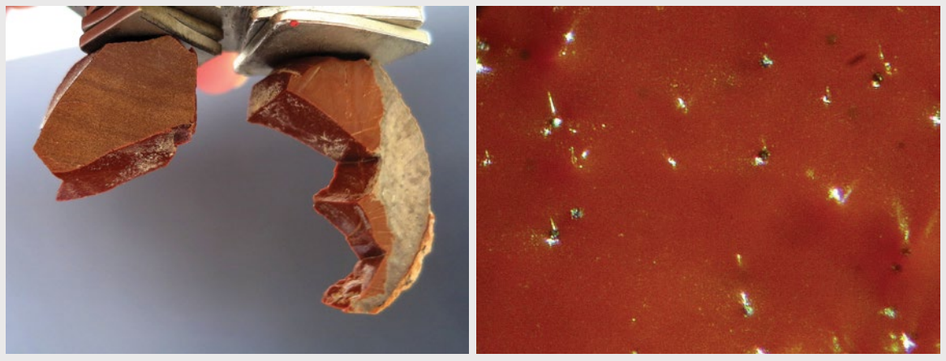

Figure 16. Left: Ethiopian Shewa opal nodule fragments supporting their weight magnetically.

Figure 17: Right: Shewa magnetic opal fracture fragment in oblique incident illumination, showing abundant minute square (presumably magnetite) pseudomorphs probably after pyrite, field of view about 1 mm.

A similar effect of reduced voidage, in a regularly stacked array within filling of voids by smaller particles, was detected in 1978 by Dr John V. Sanders, then of CSIRO, when he observed a region of dense packing in an ordered sphere microstructure in a Brazilian opal fragment furnished by the author. This was reported in *Nature* and was also illustrated on the front cover of that issue (Sanders and Murray, 1978). This observation of dual sphere sizes developing coherent packing and reduced porosity volume in Brazilian opal was later confirmed by Gauthier and Fritsch (2003), and detected by them in Mexican opal (Gauthier et al., 2004).

Porosity or voidage considerations

Conversely, a less-densely packed array, such as of an essentially BCC or simple cubic configuration, can display an increased extent of continuous porosity or voidage, as illustrated in the enhanced TEM photomicrograph of long-range ordering of Coocoran opal from Lightning Ridge (Figures 14 and 15). It shows extensive and undistorted but less than close-packed BCC stacking across a [100] plane with abundant interconnected voidage, although the microstructure still has a few minor BCC stacking defects, including localised close-packing. A scanning electron microscope (SEM) image of Javanese opal in Sun et al. (2009), reveals a very open structure with poorly consolidated packing and substantial interconnected voidage.

A notable instance of highly absorbent and interconnected voidage occurs in one specific dark brown sawn nodule of Ethiopian Shewa opal. Firstly, fragments of one half (both portions shown in Figure 4a) displayed quite distinct ferromagnetism, being able to support their entire own weights magnetically (Figure 16) on a REE magnet.

This effect was attributed to dispersed minute square pyrite crystals that had oxidised to magnetite (Hu et al., 2006; Trethewey and Chamberlain, 1988) via the intrinsic opal porosity (Figure 17) permitting moisture and oxygen access, and possibly also accounting for the limonitic brown colour of the opal.

Additionally, the sawn surface of an intact (but fractured) half of this nodule was so markedly absorbent, that when it was wet across its surface the water was rapidly absorbed in seconds leaving an apparently dry surface. A series of photomacros of this effect was taken at intervals of about only three to five seconds, as the nodule changed from being covered with a film of free liquid to being apparently "dry" within less than a half minute (Figure 18 ,1-6).

A small portion of translucent to opaque Welo light opal with a POC (Figure 19,1-6) was

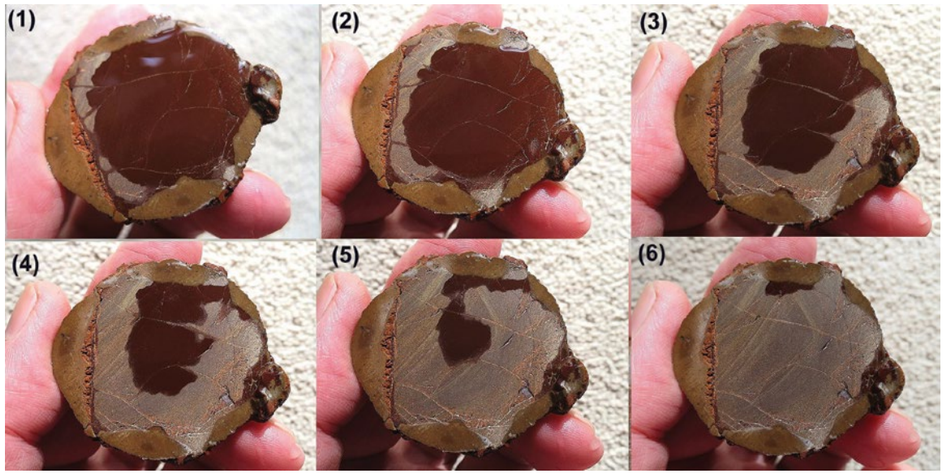

Figure 18, 1-6. Sawn (magnetic) Shewa potch opal nodule (of Figures 16 and 17) showing its exceptional rapidity of absorbency in changing from wet to apparently dry in less than half a minute, photomacros taken at about three to five second intervals.

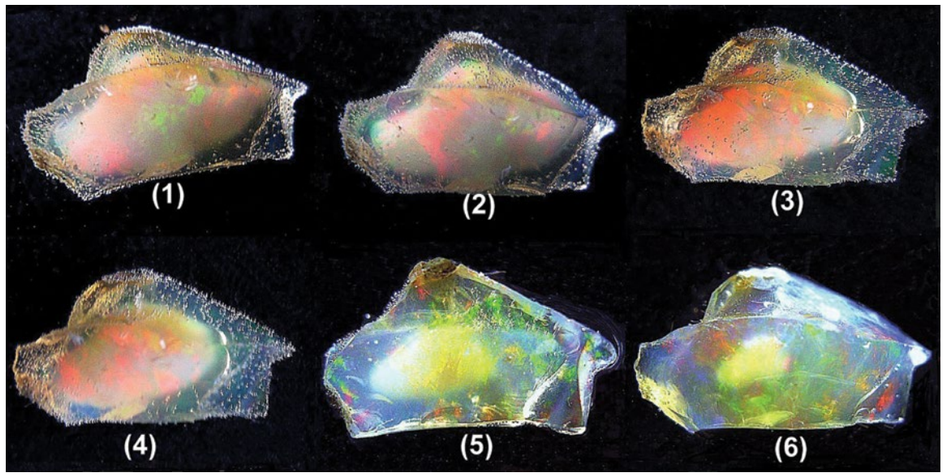

Figure 19, 1-6. Portion of Welo light opal immersed in water, showing the progressive displacement of air in the voidage by water, transforming the opaque white core zone into the transparent saturated periphery but with a weaker POC. Images exposed at about 15 minute intervals.

similarly absorbent, although not so rapidly. It was immersed in water and photomacros were exposed at about 15 minute intervals. The displaced air is apparent as myriads of minute adherent bubbles and the extent of liquid-water penetration is delineated by the junction of the transparent peripheral saturated zone and the remnant opaque zone of air-occupied voidage.

The extent of voidage in packed sphere arrays can also be significantly reduced if the spheres are compressed and deformed against each other into partial or even complete polyhedroids (see the "compressed" close-packed zone of Figure 11), sometimes even to the degree of closing off the voidage into separate and isolated unconnected cusp-shaped cavities, which are probably then non-absorbent. However, being an array of ordered discontinuities of appropriate spacing relative to visible wavelengths, they can still generate a diffraction POC. This was shown by Dr J. V. Sanders in the illustration of a scanned image of shadowed replica TEM micrograph of opal retrieved from the Coocoran field at Lightning Ridge (Figure 14). Sphere compression and distortion of ideal packing can lead to much decreased or essentially totally-eliminated porosity, and such a reduced scattering intensity that any POC is almost precluded, but it is associated with increased transparency.

Opal with a POC composed of packed arrays of spheroids is generally far from a perfectly regular lattice of exactly equal-sized spheres just touching at point-contact, as described in the idealised theoretical voidage calculation for these three most commonly encountered stacking sequences. The extent of voidage developed in stacked arrays can still be substantial and quite variable. In many instances, the voidage may be partially or completely infilled by silica gel of somewhat different RI to that of the spheroid array, leading to a non-porous opal, although often still with a POC.

Some natural opal possesses residual interconnected voidage which is surface accessible rather than isolated closed cavities between the spheroids that constitute the packed microstructures. This voidage can be penetrated by fluids, including gases such as air, or liquids including water and various other more-mobile solvents. Such opal is usually called hydrophane due to its capacity of absorbing water like a sponge. The reduced difference in RI between the host silica and the absorbed pore-water, compared to that between the displaced initial air and the silica, then leads to less intense scattering at the solid/fluid interface optical discontinuity. This causes significantly increased translucency, or to transparency, with the absorbed liquid, depending upon the extent of saturation of the voidage and the actual RI difference between silica and liquid.

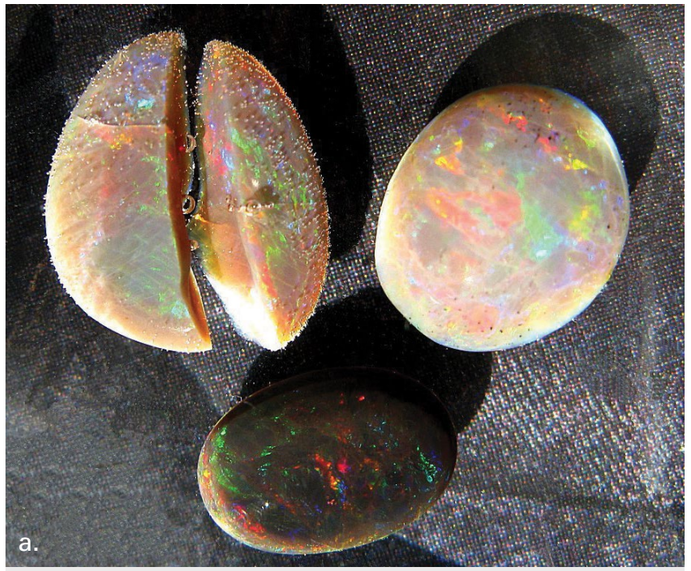

Figure 20a and b. Javanese opal specimens immersed in water for their voidage determination, causing one to instantly fracture into several fragments, presumably due to differential peripheral hydration-expansion and consequent stress development.

The reduced extent of the scattering and the increased transparency upon liquid absorption consequently reduces the intensity of any POC resulting from coherent diffraction, although the POC may actually superficially appear to be rather more intense. This is attributable to the increased transparency enabling the POC from deeper within the specimen to be visible, but was not seen when the material was more opaque. The POC is also not so diluted by the randomly scattered incident and full-spectrum white light. The actual spectral spread of any diffracted visible wavelengths of the POC is dependent upon the spheroid sizing and stacking-sequence spacing, and is independent of the extent of free voidage (Darragh and Sanders, 1965).

Porosity determination procedure

To date no estimate has been described of any actually determined vacant and surface- accessible interconnected voidage of hydrophanes. Therefore, a procedure was devised and undertaken for porous silica specimens that included the brown nodular material from Ethiopia Shewa Province and the paler opal from Welo Province. The procedure involved determining the ambient-equilibrated 'dry' mass (initially in air at 45-50% Relative Humidity (RH) at 20-21ºC), then oven air-drying at 105ºC for one hour to vaporise free adsorbed water. This water was presumed to have been captured from the ambient environment, and is retained due to the hydrophilic opaline silica being intrinsically hygroscopic (cf. silica-gel desiccant), which, together with the high surface area of its porosity, facilitates water adsorption. Hygroscopic refers to a tendency to attract and retain adsorbed moisture by polar (i.e. high surface energy) and hydrophilic ("moisture loving") materials, but without the substance dissolving in it, (then termed deliquescence).

A temperature exceeding 105ºC was deliberately avoided to minimise decomposition and irreversible thermal elimination of sensitive intrinsic-silanol functions or similar hydrous silica structures, in order to obtain a reproducible and defined baseline specimen dry-mass. It is accepted that more severe or more prolonged heating may drive off more tightly bound water until the silica eventually becomes totally anhydrous.

Specimens were desiccator-cooled, over a self-indicating silica-gel desiccant, to prevent any hygroscopic and spontaneous moisture resorption. They were then reweighed, and deliberately re-exposed to the now ambient ~ 65-70% RH atmosphere at 16-18°C for 12 hours to enable their atmospheric re-equilibration. The specimens were reweighed, and some were re-exposed for a further 12 hours to assess any additional spontaneous resorption of moisture. The atmospheric exposure at the same RH and temperature was extended for another 12 hours to a cumulative 36 hours, reweighed to assess the extent of spontaneous hygroscopic rehydration to equilibrium at the pertaining temperature and RH, and also relative to the original value prior to the oven-drying.

The rapidity and extent of the spontaneous rehydration results may have a yet unexplored but significant bearing on the extents of differential and localised swelling and contraction of specimens. This can lead to the development of the extreme stress fields that can cause opal to craze and crack. A measure of the sensitivity of a particular opal material to crazing caused by its progressive rapid and un-equilibrated drying, or to its rehydration such as by sudden immersion in water, might then be assessed. Such rapid changes in conditions could lead to localised surface expansion and development of internal stress concentration between its core and the expanded periphery that can be relieved only by progressive cracking and fracturing. However, there are undoubtedly other influencing factors.

Selected specimens were then immersed in water to displace the air which occupies continuous voidage; the immersion was prolonged for at least 24 hours beyond the time of its visible complete saturation. Total saturation was indicated by development of uniform clarity, and the elimination of the "cotton-wool" central opaque white core of undisplaced voidage air. Saturation generally occurred within about an hour (see Figure 19 of progressive water absorption of Welo opal with exposures at about 15 minute intervals). Surface-only free-liquid moisture was removed by carefully but quickly wiping with absorbent tissue, to minimise any capillarity extraction of voidage-infilling water. The saturated specimen was then rapidly reweighed before any spontaneous drying could occur. An Archimedes hydrostatic determination of the specific gravity (SG) of the water-saturated porous specimen was also promptly conducted in pre-boiled and de-aerated cooled water.

The difference between the mass of the 105ºC oven-dried specimen and its initial atmospherically-equilibrated mass gives a measure of the amount of reversibly "physisorbed" free water (not of "chemisorbed" moisture incorporated as unstable functional groups), which is adsorbed hygroscopically and retained at the ambient temperature. It is recognised that this value is probably variable and dependent on the pertaining relative humidity (RH). This is a measure of the amount of water vapour in the atmosphere as a proportion of the maximum the atmosphere can hold before it becomes saturated and condensation occurs ("dewpoint") at that temperature, (i.e. 100% RH). The oven-dried mass of the specimen gives a reproducible "zero baseline" value upon which subsequent calculations can be based. The progressive moisture absorption and desorption (either spontaneously or by oven-induced drying) is usually associated with minor shrinkage and swelling of the affected zones of the opal, so that severe stressing could be expected to be locally developed between the expansion or contraction affected peripheral zones and its less-affected core. This could lead to crazing and fracture, since (brittle) opal cannot significantly distort and stretch to accommodate localised changes in dimensions.

It has been indicated that this stress development might be directly visualised under crossed polars when the stress-strain isochromes or colour-fringes of anomalous birefringence (ABR) would map the intensity and distribution of the stress field (*pers. comm. Dr D. B. Hoover*). A conveniently flattish flake of porous oven-dried Welo opal (coded "Crystal.POC, ABR") and a dry Javanese hydrophane cabochon were water-immersed and observed between crossed polars on the stereomicroscope. An attempt was made to follow and photograph the generation of any anomalous strain birefringence (ABR) as water was absorbed and the localised saturation-transparency altered. Generation of the ABR isochromes, (coloured strain fringes), was not observed, although a uniform dark-crimson interference colour developed in the aqueous-penetrated peripheral zone of both investigated opal portions that indicated the probable development of severe stress which could cause cracking and fracture.

Conversely, the deliberate immersion directly into water of a dried hydrophane cabochon of the Javanese grey opal to determine its porosity caused it to shatter, shown in the stereomicroscope image of it still submerged in-situ (Figure 20a and b). This is consistent with the detection of the uniform crimson strain polarisation colour of the other (intact) similar Javanese cabochon.

Procedure rationale and results significance

The methodology employed in the porosity determination is described. Oven drying eliminates the specimen's variable content of pre-existing free-liquid adsorbed moisture, enabling determination of baseline silica dry-mass values for subsequent calculations. Prolonged immersion of the specimen allows absorption of water to fill the voidage, so that after removing the external water film, the mass of the saturated specimen minus that of its dry silica content gives the mass of the water occupying its voidage. The density of the water in grams per cubic centimetre is known (and is numerically equal to unity in the CGS units-system, and to its specific gravity relative to water, at least to the precision available in the procedure). The hydrostatic SG is also known, the mass of the water in grams being equivalent to the voidage volume in cubic centimetres. The hydrostatic SG determination in water of the saturated specimen, and the already known mass of the saturated fragment, allow determination of its bulk volume V in cubic centimetres (cm^3) using the formula for the definition of density, i.e. D=m/V where D is density (in g/cm^3), and m is its mass in grams (g). The voidage volume can be calculated as a proportion or percentage of the total saturated-specimen bulk-volume, giving its overall volume "porosity". The tedious repetitive calculations are easily conducted by spreadsheet. The volume of the silica phase is available from the difference between the overall volume of the saturated specimen and the volume of the saturation water. The mass of the silica itself is known from its oven-dried value, allowing calculation of the silica density by D=m/V. The comparative volume-porosity values and silica densities of the various porous materials can then be compared. In addition, the amounts and rates of spontaneous atmospheric moisture resorption at ambient RH and temperature in 12 hour intervals to 36 hours, are available for comparison and correlation with origin, porosity and silica density of the various hydrophane materials. Silica density is known to vary with the nature of the silica phase, whether any of the "A", "C" or "CT" phases defined by Jones and Segnit (1969) or with other crystalline phases such as quartz or mogánite. Comparison of these factors may enable a possibility of further characterising the different properties of hydrophane opals, such as any crazing propensity.

Experimental materials

An assortment of potentially porous materials was selected for comparative experimental evaluation of their surface-accessible voidage, or "porosity", the common alternative term. However, it should be noted that "porosity" is a misleading term as it suggests specific "pores" or holes and channels which are actually inherently foreign to the material, although the spheroidal opaline arrays possess intrinsic voidage between the packed spheroids. This voidage "porosity" can be responsible for absorption of liquids, and is cause for concern in commercial gems fashioned from the light-coloured but absorbent Ethiopian "Welo" opal in particular. It may become contaminated and discoloured by many different environmental substances that can potentially be absorbed, such as coffee, oils or perspiration or similar contaminants.

Figure 21a and b. Left: Dual portions of Shewa "magnetic" opaque potch hydrophane, as in Figures 16 and 17, used for porosity determination. Discontinuities displayed on the exposed glossy fracture surface reflect the presence of numerous magnetite cubic pseudomorphs after pyrite (see also Figure 17).

Right: Eight fragments of Mexican opal consisting of chalky to vitreous and opaque to translucent portions, several with weak POC, for porosity determinations.

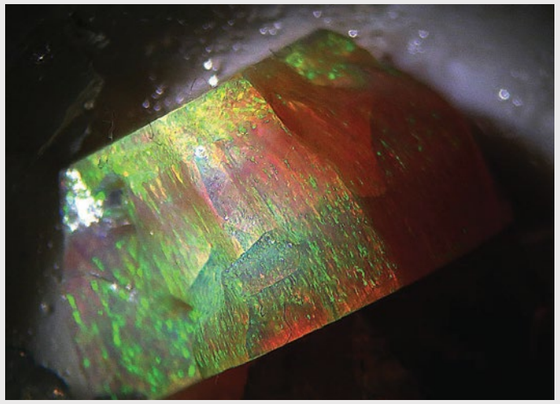

Figures 22a and b. Fragments of synthetic opal arrays prepared from TEOS by the hydrolytic technique of Stober et al. (1968). Left: Dry fragments in air. Right: The larger of the two fragments immersed in xylene to decrease its general light scattering and opacity and allowing the weak diffraction POC on and just below its surface to be seen. Specimen size 1-2 cm.

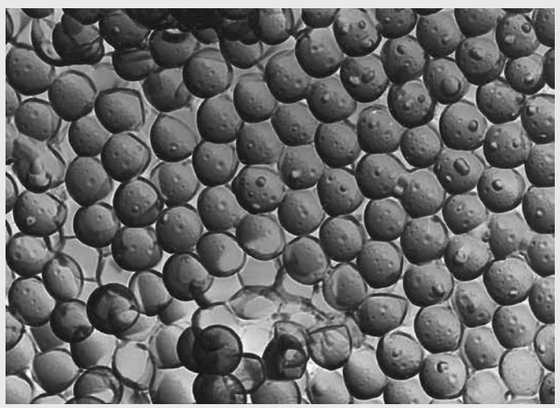

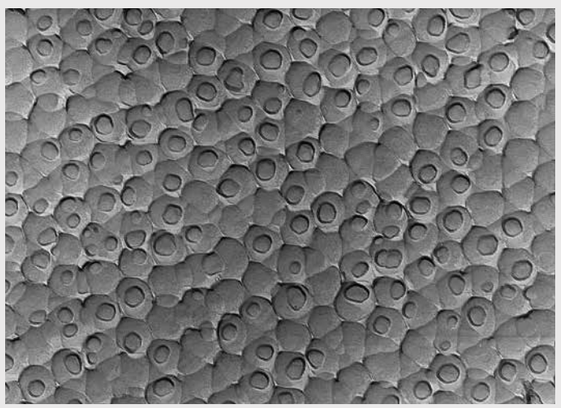

Figure 22c. Left: Shadowed TEM replica micrograph of a fracture surface of the synthetic weak- POC opaline silica close-packed spheroidal array prepared by the author as in Figures 22a and 22b, showing minute "dimples" of almost just point-contact with a previously just-touching additional layer of spheroids, indicating appreciable interspheroidal porosity.

Figure 23. Right: As in Figure 22c, but displaying rather larger contact "dimples" of a more compacted synthetic silica array.

"Bohemian cachalong" silica, Javanese dark opals, fragments of Mexican brown to pinkish opal (Figure 21a and b), and two pieces of synthetic opaline-type silica with weak POC were included (Figures 22a-c and 23). These last specimens were earlier prepared using the technique described by Stober et al. (1968). Examples of non-commercial hydrophanes have also been recovered from some minor occurrences in the USA, such as Rainbow Ridge in Nevada (wood-opal), as well as in the present-day Czech Republic ("Bohemia") where "Bohemian cachalong opal" has been recovered. Cachalong opal is a non-gem chalky-white and reputedly highly absorbent opaline silica, apparently usually occurring as botryoidal layers on igneous host rocks.

Moisture resorption is expressed as a percentage of the moisture initially lost during the oven drying at 105°C. Water resorption of several of the Ethiopian Welo samples was discontinued after the first 12 hours as they were then utilised for alternative immersion- saturation and porosity determinations (coded "NA, Immsn").

Results

Origin location	Shape, colour and texture	Silica density g/cm³	Porosity % by Vol	Init. H_2O loss, 105°C % of dry wt.
Ethiopia, Welo	Grey {A}	2.18	23.7	3.398
Ethiopia, Welo	White	2.15	17.6	2.378
Ethiopia, Welo	White	2.19	23.7	2.396
Ethiopia, Welo	White	2.15	17.3	2.752
Ethiopia, Welo	Grey, (FragEx{A})	2.19	25.9	3.667
Ethiopia, Welo	Opaque White	2.15	16.0	1.860
Ethiopia, Welo	Black	2.11	18.0	1.749
Ethiopia, Welo	Grey	2.20	24.0	2.993
Ethiopia, Welo (exTC)	"Crystal Opal", POC	2.19	27.3	2.845
Ethiopia, Welo (exTC)	"Crystal Opal", POC	2.23	29.5	5.524
Ethiopia, Welo, Transpt	"Crystal", POC, (ABR)	2.23	33.9	5.328
Ethiopia, Shewa	Med. Brown, (exDaz)	2.17	26.4	5.168
Ethiopia, Shewa. Mag	Opaque Brown	2.26	33.0	5.725
Ethiopia, Shewa. Mag	Opaque Brown	2.29	34.5	5.964
Somalia	Med. Brown, (exDaz)	2.10	6.70	2.759
Java, Indonesia	Irregular Fractd. Grey	2.28	34.3	4.395
Java, Indonesia	Oval Grey	2.26	33.8	4.160
Java, Indonesia	Oval Black ("Tea Opal")	2.12	4.17	1.418
Mexican, Opaque	Pink, Chalky	2.21	38.1	1.741
Mexican, Transpt	Lt. Brown, Glassy	2.03	0.24	0.031
Mexican, Transpt	Orange & White	1.97	1.91	0.093
Mexican, Transpt	Orange, Glassy	2.02	1.05	0.073
Mexican, Opaque	Pinkish, Vitreous	2.16	2.14	0.024
Mexican, Opaque	Pinkish, Chalky	2.20	36.5	1.427
Mexican, Transpt	Orange, Glassy	1.95	0.33	0.048
Mexican, Opaque	White, POC	1.92	2.99	0.390
Bohemian Cachalong	Opaque White	2.49	8.49	0.050
Synthetic, GMP	Chalky White	2.19	27.4	0.040
Synthetic, GMP	Chalky White	2.19	27.6	0.017

Table 1. Silica density, opal porosity % by volume, and water loss on initial oven-drying at 105°C for one hour as a percentage of the resulting silica 105°C dry-mass.

Origin Location	Shape, colour and texture	H_2O Loss,105°C, 1 hr % of dry wt.	Water resorption 12 hrs, % of dry wt.	Water resorption 24 hrs, % of dry wt.	Water resorption 36 hrs, % of dry wt.
Ethiopia, Welo	Grey {A}	3.398	2.974	NA, Immsn	NA, Immsn
Ethiopia, Welo	White	2.378	1.517	NA, Immsn	NA, Immsn
Ethiopia, Welo	White	2.396	2.292	NA, Immsn	NA, Immsn
Ethiopia, Welo	White	2.752	1.766	NA, Immsn	NA, Immsn
Ethiopia, Welo	Grey, (FragEx{A})	3.667	3.633	NA, Immsn	NA, Immsn
Ethiopia, Welo	Opaque White	1.860	1.237	1.651	1.679
Ethiopia, Welo	Black	1.749	0.804	1.613	1.626
Ethiopia, Welo	Grey	2.993	2.756	3.234	3.261
Ethiopia, Welo (exTC)	"Crystal Opal", POC	2.845	3.039	3.310	3.427
Ethiopia, Welo (exTC)	"Crystal Opal", POC	5.524	4.712	5.314	5.432
Ethiopia, Welo, Transpt	"Crystal", POC, (ABR)	5.328	5.196	5.679	5.819
Ethiopia, Shewa	Med. Brown, (exDaz)	5.168	3.761	5.013	5.101
Ethiopia, Shewa. Mag	Opaque Brown	5.725	5.342	6.462	6.939
Ethiopia, Shewa. Mag	Opaque Brown	5.964	5.649	6.812	7.011
Somalia	Med. Brown, (exDaz)	1.875	0.536	0.691	0.733
Java, Indonesia	Irregular Fractd. Grey	4.395	4.745	5.368	5.368
Java ,Indonesia	Oval Grey	4.160	4.807	5.523	5.455
Java, Indonesia	Oval Black ("Tea Opal")	1.418	0.336	0.784	0.896
Mexican, Opaque	Pink, Chalky	1.741	1.712	1.887	1.896
Mexican, Transpt	Lt. Brown, Glassy	0.031	0.031	0.010	0.010
Mexican, Transpt	Orange & White	0.093	0.060	0.053	0.053
Mexican, Transpt	Orange, Glassy	0.073	0.061	0.024	0.012
Mexican, Opaque	Pinkish, Vitreous	0.024	0.048	0.000	0.000
Mexican, Opaque	Pinkish, Chalky	1.427	1.636	1.750	1.769
Mexican, Transpt	Orange, Glassy	0.048	0.096	-0.024	-0.024
Mexican, Opaque	White, POC	0.390	0.341	0.097	0.097
Bohemian Cachalong	Opaque White	0.050	0.151	0.151	0.151
Synthetic, GMP	Chalky White	0.040	0.050	0.030	0.040
Synthetic, GMP	Chalky White	0.017	0.025	0.000	-0.008

Table 2. Moisture loss on oven-drying for one hour at 105°C of atmospherically-equilibrated opal samples (initially equilibrated at an ambient 20-21°C and ~ 45-50% RH), showing the water loss as a percentage of the resulting silica dry-mass. The extent of atmospheric resorption after cumulative periods of 12 hours, 24 hours and 36 hours subsequent exposure is shown at the lower ambient temperature of 17-18°C and a greater RH of ~ 65-70%.

Origin location	Shape, colour and texture	H_2O loss, 105°C, 1 hr % of dry wt.	H_2O resorption, 12 hrs as % of H_2O 105°C - lost	Cum. H_2O resorption, 24 hrs as % of H_2O 105°C - lost	Cum. H_2O resorption, 36 hrs as % of H_2O 105°C - lost
Ethiopia, Welo	Grey {A}	3.398	87.5	NA, Immsn	NA, Immsn
Ethiopia, Welo	White	2.378	63.8	NA, Immsn	NA, Immsn
Ethiopia, Welo	White	2.396	95.7	NA, Immsn	NA, Immsn
Ethiopia, Welo	White	2.752	64.2	NA, Immsn	NA, Immsn
Ethiopia, Welo	Grey, (FragEx{A})	3.667	99.1	NA, Immsn	NA, Immsn
Ethiopia, Welo	Opaque White	1.860	66.5	88.8	90.3
Ethiopia, Welo	Black	1.749	46.0	92.2	92.9
Ethiopia, Welo	Grey	2.993	92.1	108.1	109.0
Ethiopia, Welo (exTC)	"Crystal Opal", POC	2.845	106.8	116.4	120.5
Ethiopia, Welo (exTC)	"Crystal Opal", POC	5.524	85.3	96.2	98.3
Ethiopia, Welo, Transpt	"Crystal", POC, (ABR)	5.328	97.5	106.6	109.2
Ethiopia, Shewa	Med. Brown, (exDaz)	5.168	72.8	97.0	98.7
Ethiopia, Shewa. Mag	Opaque Brown	5.725	93.3	112.9	121.2
Ethiopia, Shewa. Mag	Opaque Brown	5.964	94.7	114.2	117.5
Somalia	Med. Brown, (exDaz)	1.875	28.6	36.8	39.1
Java, Indonesia	Irregular Fractd. Grey	4.395	108.0	122.1	122.1
Java, Indonesia	Oval Grey	4.160	115.6	132.8	131.1
Java, Indonesia	Oval Black ("Tea Opal")	1.418	23.7	55.3	63.2
Mexican, Opaque	Pink, Chalky	1.741	98.3	108.4	108.9
Mexican, Transpt	Lt. Brown, Glassy	0.031	100.0	33.3	33.3
Mexican, Transpt	Orange & White	0.093	64.3	57.1	57.1
Mexican, Transpt	Orange, Glassy	0.073	83.3	33.3	16.7
Mexican, Opaque	Pinkish, Vitreous	0.024	200.0	0.00	0.00
Mexican, Opaque	Pinkish, Chalky	1.427	114.7	122.7	124.0
Mexican, Transpt	Orange, Glassy	0.048	200.0	-50.0	-50.0
Mexican, Opaque	White, POC	0.390	87.5	25.0	25.0
Bohemian Cachalong	Opaque White	0.050	300.0	300.0	300.0
Synthetic, GMP	Chalky White	0.040	125.0	75.0	100.0
Synthetic, GMP	Chalky White	0.017	150.0	0.00	-50.0

Table 3. Moisture loss on oven drying for one hour at 105°C of atmospherically-equilibrated opal samples (initially equilibrated at an ambient 20-21°C and ~ 45-50% RH), showing the water loss as a percentage of the resulting silica dry-mass. The extent of atmospheric resorption after cumulative periods of 12 hours, 24 hours and 36 hours at the lower ambient temperature of about 17-18°C is shown, and a greater RH of ~ 65-70%.

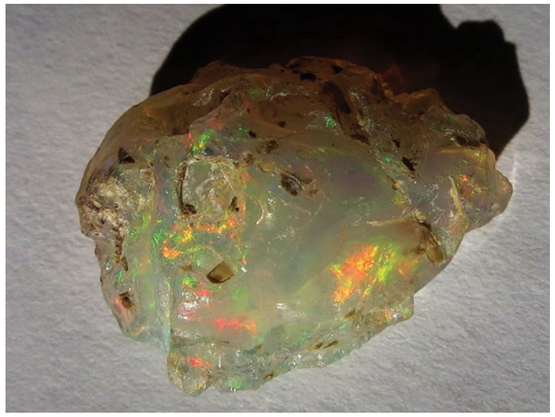

Figure 24. Welo "Crystal-ABR" specimen, showing the surface-reaching cavity-perforations that could retain water during its nominal surface removal, and which then reports as an erroneous excessive voidage. Specimen is about 15 mm across.

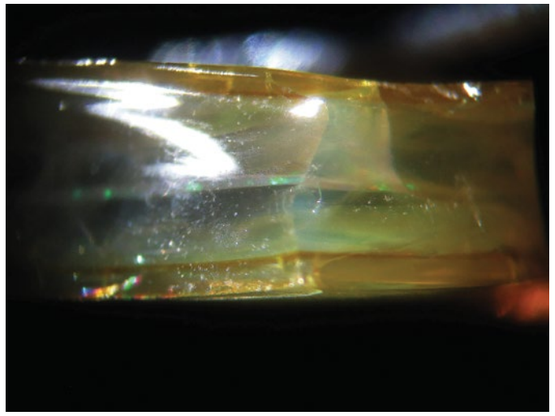

Figure 25. Somalian pale-brown potch seam opal with central thin weak-green POC band.

Discussion and interpretation

Porosity and comparison with ideal-packing voidage, oven-dehydration and moisture resorption rate and extent.

The silica materials from different locations showed quite different ranges of porosity with the Ethiopian Welo opal ranging between 16 and 30%. Of the ten Welo fragments investigated, four clustered between 16 and 18%, and six were between 23.7 and 29.5% clustering mostly around 24%. These results suggest there may be two different distinct varieties or populations of Welo materials with different absorbencies and characteristics, perhaps even from different locations.

One specimen, the Welo, "Crystal-ABR" test portion, recorded an apparently anomalous 33% voidage, but it contained a number of surface blind-perforations that probably did not have their water contents fully removed by the absorbent-tissue stage (Figure 24). That free water would therefore report as an erroneously excessive porosity. It is acknowledged that the occurrence of any such inaccessible pockets of unremoved water on the surface of a specimen is a difficulty with this method, as such remnant free-surface liquid will report as absorbed water, resulting in an over-estimated porosity.

The three tested Shewa fragments, included duplicates from the same nodule portion ("magnetic potch") that gave consistent porosities of 33.0% and 34.5%, with 26.4% for the other fragment. However, this large porosity value was obtained from quite limited and unrepresentative sampling of Shewa material, but it is also quite comparable to the 16% to about 30% voidage determined in the Welo opal. In parallel with the Mexican material and the low porosity of its glassy specimens, the range of porosity values of some of the more "glassy" translucent to transparent varieties of the Shewa opal are presently not known, but are expected to be significantly lower.

It was noted though, that the porosity of the quite similarly appearing portion of translucent pale brown opal purportedly originating in Somalia (Figure 25) was substantially less at 6.7%, but still qualifying this material as hydrophane.

This translucent Somalian specimen of seam opal was mostly without a POC except for a thin central band of green, seen stereomicroscopically during immersion. The difference between its porosity and those of the few Shewa samples of similar appearance, and the fact that it was seam opal rather than nodular, appears to substantiate the provider's claim that it was not Ethiopian, but from an undisclosed Somalian location.

Perhaps coincidentally, but interestingly, the dual fragments of the same portion of the synthetic opal array also develop porosities at 27.4 and 27.6%. This is in the same range as the Shewa specimens, and more than half of the tested Welo samples had the same range of porosity, suggesting that there may be a particular significance for this level of voidage.

It is noted that the ideal close-packed FCC configuration has a theoretical voidage of 26%, very similar to the larger range of one population of the clustered porosity values of the Welo, the Shewa and synthetic opals. The BCC configuration has an ideal voidage of 32%, close to the values for the Javanese grey specimens at 34.3 and 33.8%, as well as approaching the porosity values for the two most porous Mexican opal specimens at 38.1 and 36.5%. It is not known whether these similarities are coincidental or represent different predominating spheroidal packing configurations. Other factors may include imperfect stacking, and spheroid compaction into polyhedroids. Without some of polyhedroid compaction, the arrays would be unable to maintain physical integrity and cohesion, and lack of compaction with only the spheroidal point-contacts would lead to weak and powdery friable silica aggregation.

By comparison, the surprisingly mechanically well-consolidated and mechanically brittle "Bohemian" cachalong non-POC silica of similar appearance and chalky texture to the synthetic opal, develops porosity of only a modest 8.49%. However, its microstructure is presently uncertain. Consequently, the nature of its voidage is also unknown, whether being porosity between an array of spheroids or due to some other absorbent microstructure. Its apparently anomalous greater silica density of 2.49 g/cm^3 compared to the more typical 2.1 to 2.2 g/cm^3 of the other opal varieties (and typically from 2.10-2.13 g/cm^3 of Australian opal (Pearson, 1985), suggests that its microstructure may not be predominantly amorphous and opaline, but may contain a substantial degree of crystallinity. This structure could arise from contents of various denser microcrystalline silica polymorph phases such as quartz/

quartzine – a type of chalcedony (density 2.65 g/cm^3), cristobalite (2.27 g/cm^3), tridymite (2.28-2.33 g/cm^3) and even mogánite (2.55 g/cm^3, calculated). The minute loss upon oven drying of only 0.05% suggests that its extent of intrinsic hydration is also extremely small and probably inconsistent with a hydrous opaline-silica microstructure, and is more akin to microcrystalline quartz or a porous chalcedony.

The cachalong was also observed to not become translucent to transparent upon water immersion and saturation, suggesting that its RI is significantly greater than that of the Welo hydrophane opals. It parallels the behaviour of the synthetic material which similarly retains its opacity upon water saturation and also has only a minute oven-drying loss of just 0.02 to 0.04%, although the synthetic product does develop a density more consistent with genuine natural opal at 2.19 g/cm^3 rather than the higher 2.49 g/cm^3 of the cachalong. However, it has been experimentally observed that the dry synthetic opal arrays become translucent to almost transparent in tetrahydronaphthalene (THN or tetralin), a higher-RI colourless solvent of RI=1.545. However, they are only partially translucent when experimentally saturated with TEOS (tetraethyl-orthosilicate of RI=1.382), compared with water of RI=1.333 in which most of the Welo hydrophane opals become quite transparent and even lose much of their POC. The cachalong properties of the comparatively high value of its SG and its apparent RI (by its liquid immersion transparency effect) seem to be unusually anomalous compared to genuine natural opal, especially regarding its calculated density which is unlike the densities of almost all of the other tested opaline silica specimens and approaches even quartz's 2.65 g/cm^3.

The consistency of the essentially duplicate determinations of the synthetic opal material at 27.4 and 27.6% also supports the general reliability of the voidage estimation procedure. This parallels the (only moderate) repeatability shown in the sequential dual determinations of 27.3 and 29.5% of the same small Welo specimen "Crystal Opal, ex TC", as well as the consistent porosities of the two Javanese grey specimens of 34.3 and 33.8%. In addition, there were two fragments of the original same (cracked) Welo portion of grey opal (listed as Welo{A} and Frag. Ex{A}). The smaller fragment is a flat thin flake compared to the rather larger and more bulky original piece, (specimens 5 and 1 respectively shown in Figure 2). Although the two specimens should be expected to show identical porosities, the thin fracture flake gave a greater apparent porosity of 25.9% compared to the 23.7% of the larger fraction, suggesting that complete saturation of the latter may not have been quite attained in the 24 hours immersion. This finding is also consistent with the extents of water lost during the oven drying, which was 3.67% for the thinner flake and only 3.40% for the larger fragment. This suggests that moisture transport through the more restricted Welo opal voidage network is comparatively slow and was incomplete in the time allowed for each instance, especially for the larger fragment, and particularly for the one hour at 105ºC of oven drying. Their silica densities, though, are basically identical at 2.18 and 2.19 g/cm^3. However, the results are generally in overall reasonable agreement for the procedure in view of its limitations and simplicity, and are considered to be acceptably credible for most hydrophane gemmological-characterisation purposes.

The two grey cabochon specimens of the three Javanese examples (Figure 5) are thought to have probably been cut and polished from the same portion of rough, and display an even porosity, averaging 34%, greater than any of the Welo materials. The Javanese black "tea opal" cabochon gave a porosity of only 4.17%. The implication of this disparity in the Indonesian specimens' voidage is obscure, but may suggest different microstructures and degrees of spheroidal compaction, or perhaps different locations for the recovery of the grey and black varieties, or even that the dark pigment occupies and reduces a significant proportion of the voidage.

There were eight fragments of Mexican opal (Figure 21b) tested for porosity, of which two had pinkish-brown, opaque and chalky textures, although both displayed weak POC, especially when immersed. These two fragments also exhibited the greatest porosities determined, being 38.1 and 36.5%. The six remaining vitreous and surface specular-reflective Mexican fragments had very minor porosities of less than 3%. The exact origin of each of these diverse fragments is uncertain, and the reasons for the differences in their textures and absorbency properties are similarly obscure. However, it is evident that the porosity range of the Mexican opal material is the widest of the opal varieties investigated.

Unquantified large differences were observed in the rates of water absorption between the Welo specimen (Figure 19) and the sawn but opaque Shewa magnetic potch nodule (Figure 18). The former required more than an hour to develop its saturation transparency, whereas the Shewa nodule absorbed surface liquid in less than a minute to present an apparently "dry" surface. This occurred despite both materials showing substantial high extents of voidage (about 27% for the Welo specimen and 34% for the Shewa opal nodule). The cause of the water absorption rate difference is uncertain, although it is speculated that the Shewa rapidly-absorbent nodular opal may have much larger pore structure than the Welo material, but that inference could only really be confirmed by sub-optical microscopic inspection, such as with an SEM.

The dehydration and rehydration behaviours of the various varieties of opal were quite different, both in the extent of water lost during their 105ºC oven drying and in their resorption of water vapour from the atmosphere (Tables 1 and 2). The nominally initially air- dry and atmospherically-equilibrated hydrophane varieties, including the Welo and especially the Shewa Ethiopian opal specimens, as well as the two Mexican porous samples and the two Javanese grey hydrophane examples, all lost significant water contents of between about 2% to almost 6% on drying at 105ºC. However, the rate and extent of resorption also varied, and about two-thirds to all of the oven-drying moisture loss was regained within only 12 hours of re-exposure to ambient conditions, although at a slightly lower ambient temperature (16-18ºC) and a higher RH (between about 65-70%) than the specimens' initial ambient equilibration before drying (ambient conditions then of about 20-21ºC and RH of 45-50%). Complete regain of the oven-dried moisture was mostly attained within 24 hours and certainly within 36 hours, there being only marginal increases in the last 12 hour period. In several instances, considerably more moisture was resorbed than was expelled during the oven drying, suggesting that the equilibrium extent of water adsorption is strongly dependent upon both the pertaining ambient temperature and the RH. These results demonstrate the comparative sensitivity to ambient RH of especially the Ethiopian materials, particularly since the water resorption at the subsequently higher RH exceeded the initial oven-drying loss, which was water adsorbed previously at the atmospheric-equilibration conditions of a lower RH of 45-50% and a higher ambient temperature (20-21ºC).

The rate of water resorption was especially rapid in the more porous materials as compared to the minimally porous specimens such as most of the Mexican examples. This indicates, perhaps not unexpectedly, that more-facile diffusional water-transport paths, through the porosity, enable more rapid moisture transfer and the equilibration of the specimens' bulk with the environment. This would also suggest that more severe moisture concentration gradients, commensurate with greater localised swelling (or conversely shrinkage), would be exacerbated in materials with lower porosity where the equilibration requires much longer to dissipate the rapidly generated and more-intense moisture concentration gradients between the atmospherically exposed surface and the core of the specimen. The core can absorb or eliminate moisture only slowly by its diffusional migration through the minimally or non-porous specimen's solid-bulk. The expected consequence could then be that less-porous opaline materials would be more susceptible to cracking from changes in ambient conditions of temperature and RH than porous materials.

A comment in an earlier paper by Jones and Segnit (1969, p. 359-360) provides an explanation and a precedent supporting this supposition, describing some observations about a portion of non-gem Lake Eyre wood-opal: *"If the major pore structure is such as not to allow the physically adsorbed water to escape freely, sudden exposure to a temperature higher than that underground will increase the pressure within the pores and develop stresses that could lead to delayed cracking. Slow movement of the opal to the surface such as was done in the old Bohemian mines (Leechman, 1961) would allow diffusion of water from the opal without undue stresses being developed. It is interesting to note here a crystalline wood-opal from Lake Eyre, South Australia (Segnit et al., 1965), which consists of a clear section with a closed pore structure and a milky part with an open pore structure; the clear portion contains abundant cracks whereas the milky material is free from cracks."*

The reasons for the substantial differences in the behaviours of the Mexican vitreous specimens which exhibited predominantly very low oven-drying losses and very small water-resorption gains, and to the two significantly porous Mexican examples with also higher moisture loss and regain properties is uncertain. It is surmised that the extent and rate of moisture transfer is related to the exposed and atmospherically accessible surface area. This would be considerably greater for the porous materials, especially since the effective surface area is not just that of the diffracting-array spheroids but also of their far more abundant composing primary micro-spheroids, as shown by Jones and Segnit, (1969, p. 360) and to which the porosity enables access.

It should also be noted that the superficially large apparent values of percentage water resorption for the synthetic opal material, and for several of the Mexican specimens, is misleading in that the amount of oven-dried expelled water is only a minute proportion of the silica dry mass. In some cases this was very close to the analytical resolution (tenths of a milligram only), so that resorption of only minute masses of water amounts to apparently excessive proportions of the initially adsorbed moisture. The synthetic material though, still has a substantial porosity, typically about 27.5% by volume, yet its oven-drying water loss and its spontaneous moisture resorption from the atmosphere are very small at the same temperature and RH as for the other natural specimens with greater moisture avidity.

These results could be interpreted differently. The diffracting array spheroids of the synthetic material may not be composed of aggregates or of concentric shells of primary microspheroids as are natural opals, so that the effective adsorbing surface is limited to only the larger-array spheroids and is therefore comparatively very low. It might also be interpreted to mean that the fundamental adsorption properties of the synthetic monodisperse silica spheroids developed by the TEOS ethanolic alkaline hydrolysis are quite different to those of natural opaline silica deposited by subterranean nucleation and growth from natural and very dilute aqueous silica sols. The reasons for the synthetic materials' anomalous adsorption and dehydration behaviour are still presently unresolved. It certainly differs in refractive index in that it is chalky-opaque even when saturated with a solvent that cause natural hydrophanes, like the Welo opal, to become transparent, such as water of RI 1.333. It is not until the penetrating solvent RI approaches about 1.545, (e.g. tetralin) that any extent of translucency is developed. However, the synthetic silica does not differ appreciably in silica density (2.19 g/cm^3) to most of the natural opal materials, except for the "Bohemian" cachalong (density 2.49 g/cm^3) but to which it is otherwise appears rather similar.

Conclusions

A water-displacement technique was devised for provisionally estimating the apparent absorbent porosity of various opaline silicas, as well as enabling determination of the actual silica density as an indicator of its possible constitution. The extent of absorbent porosity of the examined selection of silica materials ranged between effectively nil for one (vitreous) Mexican example, to in excess of 38% by volume, for another (chalky) Mexican opal portion. The porosity of the pale opal specimens from Welo, Ethiopia, seemed to fall within two distinct groups, one with voidage ranging between about 16 and 18%, and the other between 23 and 30%, clustering mostly around 24%. Whether this dual grouping is coincidental or implies distinct differences in structures or packing properties is obscure. Duplicate portions of porous brown Ethiopian (non-POC) opal from Shewa also gave porosity values of 33.0 and 34.5%, although a separately sourced fragment of the same Shewa brown opal gave only 24.5%. The duplicate synthetic opal fragments gave similar values of 27.4 and 27.8%, suggesting satisfactory reproducibility of the displacement technique, and also approximately consistent with the porosity of much of the Ethiopian opal.

Atmospherically adsorbed moisture contents of the different silica specimens, and which was thermally removable at 105ºC, also varied significantly. The subsequent rate and extent of the spontaneous moisture resorption from the atmosphere was seen to be substantially dependent upon the Relative Humidity (RH), but the final extent of regained moisture generally returned to at least if not rather greater values than the original 105ºC pre-drying level within about 24 to 36 hours under ambient exposure (at slightly higher RH and lower temperature).

A significant variation in the densities of the various types of opaline silicas was also observed, ranging from apparently less than 2.0 g/cm^3 to values significantly in excess of those usually associated with opaline silica at about 2.2 g/cm^3. Values to 2.49 g/cm^3 (cachalong) even approached densities more generally associated with those of the various silica crystalline polymorphs like cristobalite, mogánite and even quartz (2.65 g/cm^3). These variations of properties of opaline silicas suggest that "opal" is not yet an entirely well characterised, uniform and homogeneous substance, but that there are many interesting variations and properties yet to be determined about its structure and nature.

Acknowledgements

Dr Don Hoover, Bear and Cara Williams (StoneGroupLabs, Missouri) are thanked for their advice and assistance with the manuscript. All photographs are by the author, references are from preprints of numerous opal publications provided originally by Dr J. V. Sanders, (then Senior Research Scientist at CSIRO, Tribophysics Dept) and all of the TEM etched and shadowed-replica micrographs of numerous opal structures, now in the author's possession, were taken by Dr J.V.Sanders (dec.) and TEM Technical Assistant, Bramwell Dawson (dec.), microscopy assistant at CSIRO in the 1960s and 1970s.

Specimens were originally from the collection of B. Shelton (Bohemian cachalong) (dec.), L. Enos (Spencer opal), Darren Arthur of DazlynGems (Mexican, Shewa and Somalian opal), S. Street (Javanese grey and black/tea opals), A. Axton (Brazilian opal with dual-size spheres), C. Whelan (Ethiopian Shewa nodules), T. Coldham (Ethiopian Welo hydrophane), Yvonne Jiew (Welo hydrophane), John Tunzi (past of QGRS) (Welo hydrophane).

References

Cullity, B.D. (1959) *Elements of X-Ray Diffraction*. (2nd edition), 79 ff p. Addison-Wesley Publishing Inc.: Reading.

Darragh, P.J., Sanders, J.V. (1965) The Origin of Colour in Opal Based on Electron Microscopy. *Gems and Gemology,* **11**(10), pp. 291-298.

Darragh, P.J., Sanders, J.V. (1969) Volcanic gem opals: the result of an examination by electron microscope. *The Australian Gemmologist*, **10**(8), pp. 5-8.

Gardner, M. (1960) Reflections on the Packing of Spheres. Mathematical Games column. *Scientific American*, May-June.

Gauthier J.-P., Fritsch E. (2003) Une rareté structurale: l'opale noble bidisperse. *Revue de Gemmologie a.f.g.*, No. **148**, pp. 32-35.

Gauthier J.-P., Fritsch E., Barreau A., Aguilar-Reyes B., Lasnier B. (2004) Phase de Laves dans la première opale CT bidisperse. *Comptes Rendus de l'Académie des Sciences – Géosciences*, **336**(3), pp. 187-196.

Hoover, D.B., Yohannes, T.Z., Collins, D.S. (1996) Ethiopia, A New Source For Precious Opal. *The Australian Gemmologist*, **19**(7), pp. 303-307.

Hu, G, Dam-Johansen, K, Wedel, S, Hansen J.P (2006) Decomposition and oxidation of pyrite. *Progress in Energy and Combustion Science*, **32**, pp. 295-314.

Jones, J.B., Sanders, J.V., Segnit, E.R. (1964) Structure of Opal. *Nature*, **204**(4962), pp. 990-991.

Jones, J.B. and Segnit, E.R. (1969) Water in Sphere-Type Opal. *Mineralogical Magazine*, **37**(287), September, pp. 357-361.

Jones, J.B. and Segnit, J. (1971) The Nature of Opal 1, Nomenclature and Constituent Phases. *Journal of the Geological Society of Australia*, **18**(1), pp. 57-68.

Moffatt, W.G., Pearsall, G.W., Wulff, J. (1964) Vol 3. *The Structure and Properties of Materials*. 29-40 p. Wiley and Sons Inc: New York.

Nassau, K. (1983) *Physics and Chemistry of Colour: The Fifteen Causes of Color*. 274-279 p. John Wiley and Sons: New York.

Pearson, G. (1985) Role of Water in Cracking of Opal. *The Australian Gemmologist*, **15**(12), November, pp.435.

Rondeau, B., Fritsch, E., Mazzero, F., Gauthier, J-P., Cenki-Tok, B., Bekele, E., Gaillou, E. (2010) Play-Of-Color Opal from Wegel Tena, Wollo Province, Ethiopia. *Gems and Gemology*, Summer 2010, pp. 90-105.

Sanders, J.V. (1964) Colour of Precious Opal. *Nature*, **204**(4964) Dec. 19, pp.1151-1153.

Sanders, J.V. (1968) Diffraction of Light by Opals. *Acta Crystallographica*, A**24**, pp. 427-434.

Sanders, J.V. and Darragh, P.J. (1971) The microstructure of precious opal. *Mineralogical Record*, **2**(6), pp. 5.

Sanders, J.V. and Murray, M.J. (1978) Ordered Arrangements of Two Sphere Sizes in Opal. *Nature*, **275**, 21 September, pp. 201-203.

Semrad, P. (2011) *The Story of European Precious Opal from Dubnik*, 174 p. Pub. Granit Ltd: Czech Republic.

Semrad, P. (2015) European precious opal from Cervenica-Dubnik – an historical and gemmological summary. *The Australian Gemmologist* **25**(11-12), pp. 372-388.

Stober, W., Fink, A., Bohn, E. (1968) Controlled Growth of Monodisperse Silica Spheres in the Micron Size Range. *Journal of Colloid and Interface Science*, **26**, pp. 62-69.

Sun, T.T., Mok, P.C., Paul, S.L., Paramita M., Arps, C.E.S., Atichat, W., Fritsch, E., Kang, W.W., Wijaya, K. (2009) Precious Opal From Java, Gemmological Properties, Micro- and Nano-Structures. *The Australian Gemmologist*, Third Quarter **23**(11), pp. 513-528.

Todor, D.M. (1976) *Thermal Analysis of Minerals*. Abacus Press: Tunbridge Wells.

Trethewey, K.R. and Chamberlain, R.J. (1988) Pearson Education Limited ed. *Corrosion for students of science and engineering*. 142 p. and 233 p. Longman: Harlow.